ELSEVIER

Journal of Materials Processing Technology 174 (2006) 389–393

Journal of Materials Processing Technology

www.elsevier.com/locate/jmatprotec

High strain rate superplasticity of a Zn–22 wt.%Al–*x* wt.%Ag alloys

Said R. Casolco [a,b,c,*], M. López Parra [a], G. Torres Villaseñor [b]

[a] *Centro de Diseño y Manufactura- FI-UNAM.,70-360, 04510 México*
[b] *Instituto de Investigaciones en Materiales, UNAM, Mexico*
[c] *Department of Mechanical Engineering, the University of California, Riverside, CA 92521, USA*

Received 26 September 2003; accepted 20 February 2006

Abstract

The present work investigated the microstructural evolution and mechanical properties of ternary Zn–22 wt.%Al–*x* wt.%Ag (*x* = 1.0 and 4.24 wt.% Ag) alloys. The aim is to advance in the understanding of the relationship that takes place between the tension at strain rates from 1×10^{-5} to $10\,s^{-1}$ at 230 °C, and silver content. The microstructure of the *x* = 1.0 wt.% Ag alloy consisted of two solid solutions, an α-aluminum solid solution and a η-zinc solid solution. In the *x* = 4.24 wt.% Ag alloy, an intermetallic $AgZn_3$ compound was present in addition to the α and η solid solutions. The presence of silver proved to have great influence on the resultant stress versus strain rate curve, which showed high values of elongation at high strain rate superplasticity (HSRS). The experimental results suggested that the origin of HSRS was related to microstructural refinement which, in turn, was produced by the silver content. The microstructures of the alloys under study were observed in deformed and undeformed samples by scanning electron microscopy (SEM), X-ray analysis was used to investigate the deformation mechanisms involved.

Keywords: Superplasticity; HSRS; Zinag; Zn–Al–Ag

1. Introduction

Superplasticity in Zn–Al alloys has been widely investigated [1,2]. Generally, superplasticity in metallic alloys is achieved at low strain rates at temperatures around $0.5T_m$ (T_m = melting temperature in K). However, recent research has demonstrated that superplasticity can exist at considerably higher strain rates ($>10^{-3}\,s^{-1}$) [2]. So far, this high strain rate superplasticity (HSRS) phenomenon has been observed mainly in metal matrix composites [3–5] and mechanically alloyed alloys [6–8], and it has also been observed in metallic alloys produced by conventional methods [9–11]. Even with such a large set of results, the mechanistic origin of this type of superplasticity is the subject of considerable debate [12]. Some researchers have concentrated in explaining the role of microstructures and parametric dependencies [13–15]. It is important to recognize that HSRS is observed in materials with second phase particles. Furthermore, based on experimental results concerning the temperature dependence of flow stress, elongation, strain rate sensitivity exponent, activation energy and cavitation in HSRS fine grain materials, it has been reported [16,17] that the deformation mechanism is related to grain boundary sliding and a special accommodation process. It is suggested that an accommodation helper, such as a liquid phase, is responsible for the observed HSRS in very fine-grained materials [16,17].

The purpose of this paper is therefore to examine the influence of the silver content (1.0 wt.% Ag and 4.24 wt.% Ag) on the Zn–Al eutectoid alloy. The investigation focuses mainly on the superplastic behavior of Zn–Al–Ag alloys. To our knowledge, this is the first investigation on superplasticity of Zn–Al–Ag alloys.

2. Experimental material and procedure

An eutectoid Zn–Al based alloy was prepared from 99.9% purity Al, special high grade Zn and 99.99% Ag, melted in a graphite crucible in air, and finally cast into a 24 mm thick ingot. Two compositions, were prepared Zn–22 wt.%Al–1.0 wt.%Ag and Zn–22%Al–4.24 wt.%Ag, which are named as "Zinag-1" and "Zinag-2", respectively. In order to produce the tensile samples of 10 mm gauge length, with the gauge length parallel to the rolling direction, ingots were warm rolled at 350 °C from 24 mm to a 1 mm thick sheet. In order to determine the superplastic behavior as a function of the strain rate, the samples were deformed at a rate of 1×10^{-5} to $10\,s^{-1}$ at constant temperature of 230 °C. After testing, selected samples were mechanically polished and the microstructure of the specimens was examined by SEM, before and after deformation. The crystallographic phase identification of the sam-

* Corresponding author. Tel.: +52 951 827 5830; fax: +52 951 827 2899.
E-mail address: sroblesc@engr.ucer.edu (S.R. Casolco).

0924-0136/$ – see front matter © 2006 Elsevier B.V. All rights reserved.
doi:10.1016/j.jmatprotec.2005.02.271

ples was carried out with a Siemens 5000 X-ray diffractometer using Cu Kα radiation.

3. Results

3.1. Microstructures

After rolling to 90% reduction at 350 °C, a very fine and uniform grain size of about 1 μm was observed Fig. 1a and b, this microstructure is very stable at room temperature. The microstructure of Zinag-1 consists of fine-grained α and η regions separated by large elongated zones of the η phase (Fig. 1a). SEM observations showed that the Zinag-2 alloy had also the ε phase ($AgZn_3$), which appeared as bright patches inside the η zones (Fig. 1b). Fig. 2 shows X-ray diffractograms of the initial material Zinag-1 and Zinag-2, after rolling at 350 °C. In bottom curve of Fig. 2 shows the presence of the aluminum solid solution (α, fcc) and the zinc solid solution (η, hcp) in the Zinag-1 alloy. The top curve of Fig. 2, shows the presence of the intermetallic phase $AgZn_3$ (ε, hcp) in Zinag-2, was established by the (0 0 2) and (1 0 1) reflections that appear at $2\theta = 41.5°$ and 42.5°, respectively.

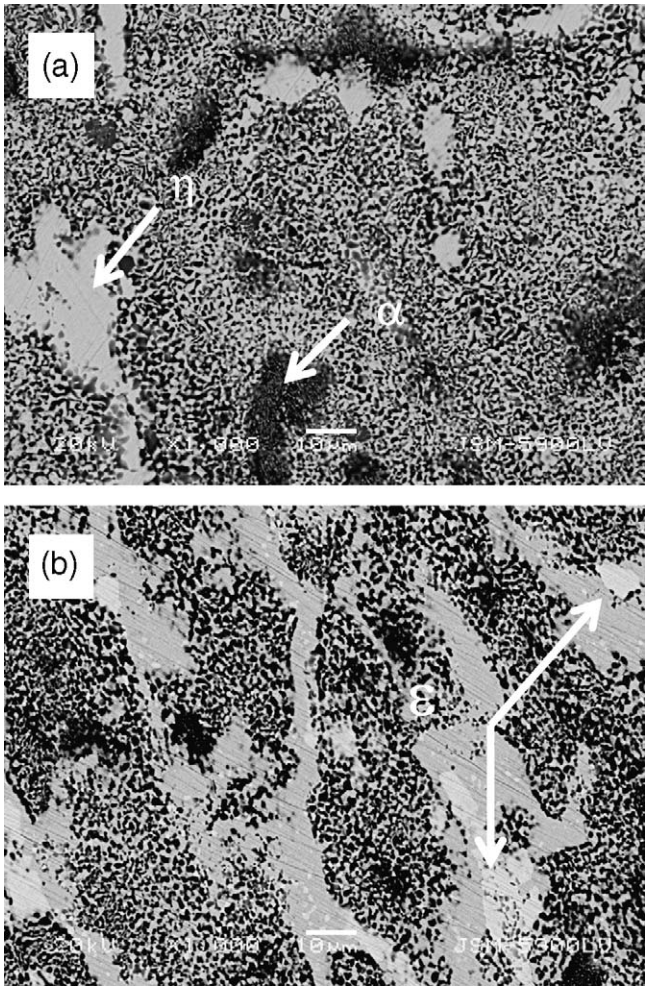

Fig. 1. Microstructure prior to the tensile test for (a) Zinag-1 and (b) Zinag-2, the ε phase is marked.

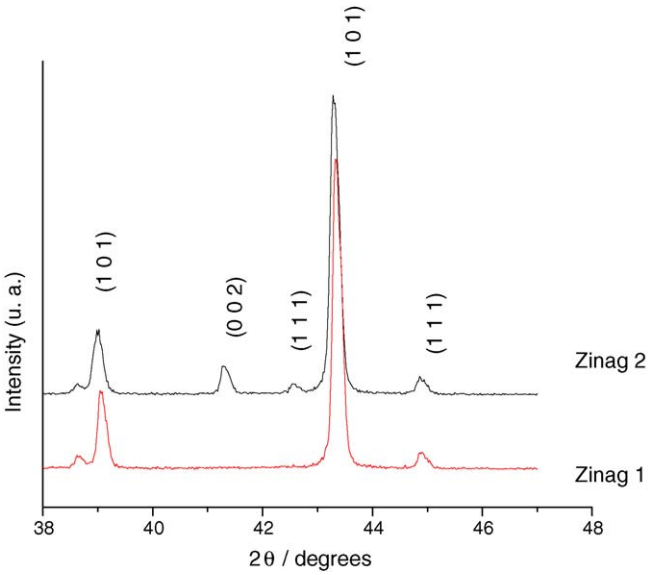

Fig. 2. XRD patterns of the Zinag-1 and Zinag-2 superplastic alloys.

3.2. Mechanical behavior

Figs. 3 and 4 show the nominal strain to fracture and the maximum flow stress in Zinag-1 and Zinag-2, respectively. Furthermore, the flow stress increases with increasing strain rate. The optimum strain rate for maximum elongation was 10 s^{-1} in both alloys indicating that this material exhibits the HSRS behavior, as observed in experiments carried out with other

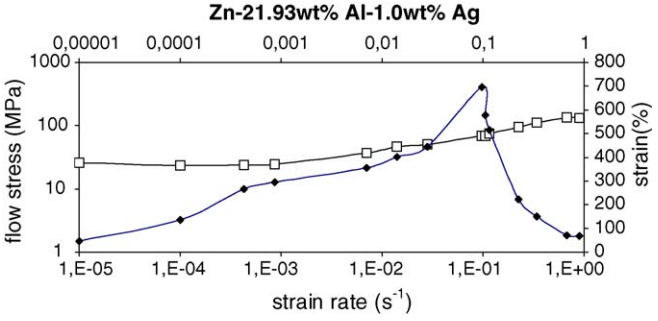

Fig. 3. Nominal strain to fracture and maximum flow stress with nominal strain rate for Zinag-1.

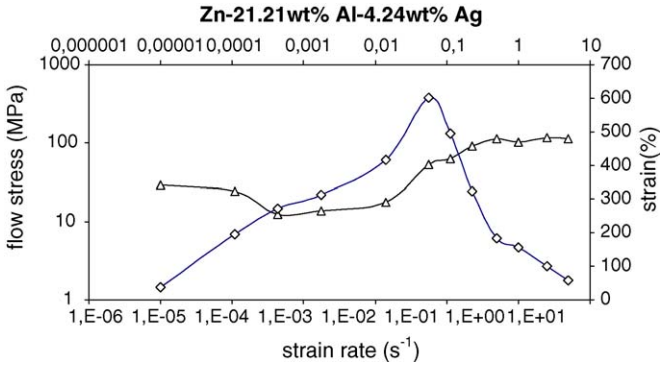

Fig. 4. Nominal strain to fracture and maximum flow stress with nominal strain rate for Zinag-2.

alloys [16,17]. The excellent properties of the Zinag alloys are attributed to a significantly refined microstructure. The stress versus strain rate curves show a kind of sigmoidal shape with regions of different values of m. Both alloys increased their strain for the maximum in the stress–strain plot with strain rate according to typical superplastic materials, following the general equation $\sigma = k\dot{\varepsilon}^m$, where σ is the flow stress, $\dot{\varepsilon}$ is the strain rate, k is a constant incorporating the structural and temperature dependences and the strain rate sensitivity m is the slope of this curve ($\mathrm{d}\ln\sigma/\mathrm{d}\ln\dot{\varepsilon}$).

In general, large elongations were obtained in the temperature and strain rate regions where high values of m were

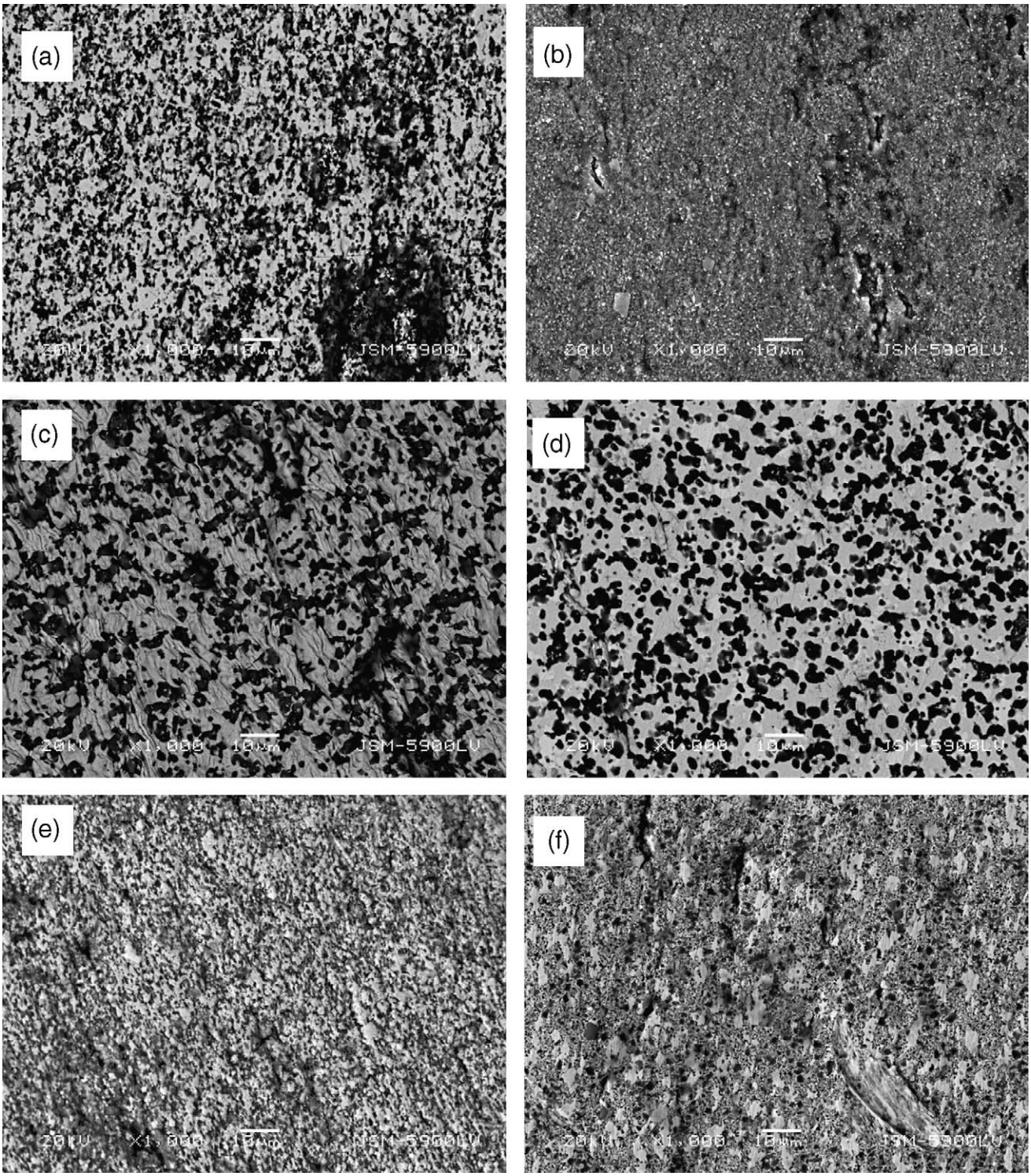

Fig. 5. The microstructures of Zinag-1 (a–c) and Zinag-2 (d–f) after deformation at 230 °C. a and d were obtained in minimum strain rate region, b and e in the superplastic strain rate region and c and f in the maximum strain rate region.

observed (Figs. 3 and 4). These can be related to the three stages of plastic flow considered by Mohamed and Langdon [1] in discussing the creep behavior of fine-grained materials (regions I–III).

The data for the fine-grained Zinag-1 was identified at the low strain rate region (Fig. 3), with 0.5 rate sensitivity. In contrast, Zinag-2 has a high silver content, and thus a high density of $AgZn_3$ phase compared to Zinag-1; it can be anticipated that there exists an appreciable region I. The theory of Nabarro–Herrings alloys explains the m value (<0.48) for region I; this is schematically illustrated in Fig. 4. This evidence was found for diffusional creep which is predicted to occur at a strain rate of about $7 \times 10^{-4}\,s^{-1}$ [16–18]. Large elongations were obtained at the high strain rate of $10^{-1}\,s^{-1}$, which coincide with the strain rate range where a relatively high value of m (>0.8) was found. Furthermore, a maximum value of about $m = 0.8$ was obtained in the high strain rate range, suggesting that grain boundary sliding is also occurring. This shows the effectiveness of silver content in evolving a microstructure amenable to HSRS. However, it should be emphasized that, even in the solid solution alloys, elongation decreases with an increase of the silver content, although the amount of elongation is not large. Additionally, HSRS is improved. Based on the above-mentioned findings, it can be stated that the grain boundary sliding of α and η phases will play an important role in the superplastic deformation. From the superplastic test result (Figs. 3 and 4), it can be inferred that solute silver also has a significant effect on superplasticity. The difference in superplastic flow characteristics between the Zinag alloys and typical superplastic materials might be attributable to differences in the microstructural evolution during deformation.

The flow stress of superplastic deformation may support this viewpoint. Changes in the microstructure during deformation, such as grain size and the morphology of grain, generally depend on the deformation mechanism. Fig. 5a and b shows the variations in the microstructure observed near the fracture region of the specimens deformed at a lower strain rate, optimum deformation and maximum strain rate. The Zinag-1 alloy after 150% deformation at a strain rate of $1 \times 10^{-4}\,s^{-1}$ (Fig. 5a) shows smaller grain size zones of the η phase mixed with equiaxed grains of α phase. In contrast, the microstructure of the Zinag-2 alloy deformed in the same way (Fig. 5b) shows a remarkable grain refinement in both phases.

Alternatively the samples that were deformed at a high strain rates, show a reverse behavior. The Zinag-1 shows a strong grain refinement (Fig. 5b) and the Zinag-2 alloy show patches of the η phase surrounded by coarse and fine equiaxed α phase grains (Fig. 5c). When deformation takes place at the maximum strain rate ($9 \times 10^{-1}\,s^{-1}$) both alloys show (Fig. 5d and e) a homogeneous distribution of the aluminum grains in the η phase matrix. A small grain growth is observed in the case of Zinag-1 (Fig. 5c) and the η phase shows some kind of fluting. This experimental evidence suggests that the flow stress increases with increasing grain size and that the deformation is more strongly controlled by the motion of the dislocations in grains. The deformation mechanism that takes place in this case facilitates this behavior. Dynamic recrystallization may occur in some grains, i.e., the growth of other grains rapidly occurs during deformation since the ε phase does not disturb the grain boundary migration.

4. Discussion

The experimental results show some remarkable differences between the alloy with the intermetallic $ZnAg_3$ phase (Zinag-2) and the alloy without it. As plotted in Figs. 3 and 4, the data in the low strain rate region reveals the presence of an important difference in the behavior of Zinag-1 with respect to Zinag-2. The region I, observed in Zinag-2 with a slope near 0.48, may be an indication of the existence of diffusional creep [19–21], as a result of diffusion at the testing temperature might be produced by the compositional changes of the ε, α and η phases.

The microstructure of the specimens deformed in the region of very high values of m (Fig. 5b and e), suggests the activation of recrystallization during deformation. In the case of Zinag-1, where two solid solutions are present, the recrystallization occurs at a slower rate than in the case of Zinag-2, where we have the presence of a third phase ($AgZn_3$). Therefore, a microstructure with fine particles of bright zinc phase is observed in Zinag-1 and a more advanced grade of recrystallization is observed in Zinag-2. This recrystallization can be explained by the high strain rate sensitivity values found in these alloys (within this range of strain rates). However, dynamic grain recrystallization has occurred which contributes to a decrease in m prior to failure. Adding $AgZn_3$ enhances the change in grain rate. This seems to be a disadvantage for the superplasticity. Nevertheless, it is confirmed that the tensile ductility is improved by adding $AgZn_3$ at the high strain rate of $10^{-1}\,s^{-1}$ [18]. In general, it can be concluded that the differences in superplastic flow behavior between the Zinag-1 and Zinag-2 are due to differences in microstructural evolution during deformation. Fig. 5f shows higher grain growth due to the strain rate that takes place in region III.

5. Conclusions

On the basis of experimental results, the origin of HSRS in Zinag alloys could be explained as follows:

1. Elongation to failure tests performed on the Zinag alloys revealed very high ductility under conditions where the strain rate sensitivity was high. Elongations of the order of ≈650% were observed at 230 °C at strain rates of $1 \times 10^{-1}\,s^{-1}$. This outcome is attributed to the presence of high strain rate superplasticity related to the microstructural refinement that takes place during the mechanical process, aided by the addition of silver.
2. The resultant stress versus strain rate curve is not a sigmoidal with its three classical zones. The addition of small amount of Ag to the eutectoid Zn–Al alloy increase the strain rate for superplasticity. These changes are produced by diffusion and recrystallization.

Acknowledgements

Authors acknowledge the technical assistance of J.M. Gómez de Salazar and J. Quiñones Diez (UCM-Spain). It is also acknowledged the financial support of DGEP-UNAM, SNI-CONACyT.

References

[1] F.A. Mohamed, T.G. Langdon, Acta Met. 23 (1975) 117.
[2] F.A. Mohamed, S.-A. Shei, T.G. Langdon, Acta Met. 23 (1975) 1443.
[3] T.G. Nieh, J. Wadswoth, Scripta Metall. Mater. 28 (1993) 1993.
[4] T.G. Nieh, C.A. Henshall, J. Wadsworth, Scripta Metall. 18 (1984) 1405.
[5] T. Imai, M. Mabuchi, T. Tozawa, M. Yamada, J. Mater. Sci. Lett. 9 (1990) 255.
[6] M. Mabuchi, T. Imai, J. Mater. Sci. Lett. 9 (1990) 763.
[7] T.G. Nieh, P.S. Gilman, J. Wadswoth, Scripta Metall. 19 (1985) 1375.
[8] T.R. Bieler, T.G. Nieh, J. Wadswoth, A.K. Mukherjee, Scripta Metall. 22 (1988) 81.
[9] K. Higashi, T. Okada, T. Mukai, S. Tanimura, Scripta Metall. Mater. 26 (1992) 761.
[10] T.G. Nieh, J. Wadswoth, in: R. Pearce, L. Kelly (Eds.), Superplasticity in Aerospace Aluminum Alloys, Ashford press, 1985, p. 194.
[11] N. Furushiro, S. Hori, Y. Miyake, Proceedings of the International Conference on Superplasticity in Advanced Materials—ICSAM-91, 1991, p. 557.
[12] R.S. Mishra, T.R. Bieler, A.K. Mukherjee, Mater. Sci. Forum 243–245 (1997) 315.
[13] R.S. Mishra, A.K. Mukherjee, Scripta Metall. 25 (1991) 271.
[14] R.S. Mishra, T.R. Bieler, A.K. Mukherjee, Scripta Metall. Mater. 26 (1992) 1605.
[15] B.Q. Han, K.C. Chan, T.M. Yue, W.S. Chan, Scripta Metall. Mater. 33 (1995) 925.
[16] K. Higashi, M. Mabuchi, Mater. Sci. Forum 243–245 (1997) 267.
[17] K. Higashi, Mater. Sci. Forum 170–172 (1994) 131.
[18] S.R. Casolco, J. Negrete-Sánchez, G. Torres-Villaseñor, Proceedings of the Congress on Dislocations Plasticity and Metal Forming, Neat press, 2003, p. 507.
[19] R.L. Cobble, J. Appl. Phys. 34 (1969) 82.
[20] F.R. Nabarro, Report of a conference on strength of solid, 1948, p. 75.
[21] C. Herring, J. Appl. Phys. 21 (1950) 437.